Scanning Microscopy

Electrical Characterization of Submicrometer Silicon Devices by Cross-Sectional Contact Mode Atomic Force Microscopy

P. De Wolf
Interuniversity MicroElectronics Centre, dewolfp@imec.be

T. Trenkler
Interuniversity MicroElectronics Centre

T. Clarysse
Interuniversity MicroElectronics Centre

M. Caymax
Interuniversity MicroElectronics Centre

W. Vandervorst
Interuniversity MicroElectronics Centre

See next page for additional authors

Utah State University
MERRILL-CAZIER LIBRARY

Electrical Characterization of Submicrometer Silicon Devices by Cross-Sectional Contact Mode Atomic Force Microscopy

Authors

P. De Wolf, T. Trenkler, T. Clarysse, M. Caymax, W. Vandervorst, J. J. Snauwaert, and L. Hellemans

ELECTRICAL CHARACTERIZATION OF SUBMICROMETER SILICON DEVICES BY CROSS-SECTIONAL CONTACT MODE ATOMIC FORCE MICROSCOPY

P. De Wolf[*], T. Trenkler, T. Clarysse, M. Caymax, W. Vandervorst, J.J. Snauwaert[1] and L. Hellemans[1]

Interuniversity MicroElectronics Centre (IMEC), Kapeldreef 75, B-3001 Leuven, Belgium
[1]University of Leuven, Celestijnenlaan 200D, B-3001 Leuven, Belgium

Abstract

Two contact mode atomic force microscopic (AFM) techniques under ambient conditions are presented for the electrical evaluation of cross sectioned silicon devices. In the first technique, a conductive AFM tip is used as a voltage probe to determine the local potential distribution on the cross section of a silicon device under operation. The electrical potential is measured simultaneously with the surface topography with nanometer resolution and mV accuracy, offering an easy way of correlating topographic and electrical features. A second method, nanometer spreading resistance profiling (nano-SRP), performs localized spreading resistance measurements to determine the spatial distribution of charge carriers in silicon structures. The conversion of the resistance profiles into charge carrier profiles as well as the applied correction factors are discussed in more detail. Both methods are used to map electrical characteristics of state-of-the-art silicon structures.

Key Words: Atomic force microscopy (AFM), potentiometry, spreading resistance profiling (SRP), carrier profiling, dopant profiling.

[*]Address for correspondence
Peter De Wolf
IMEC
Kapeldreef 75
B-3001 Leuven, Belgium
Telephone number: +32 16 281305
FAX number: +32 16 281501
E-mail: dewolfp@imec.be

Introduction

In the design and fabrication of state-of-the-art silicon devices, knowledge of basic electrical properties, such as the potential distribution under operation and the electrical carrier distribution on a nanometer-scale is of great importance. Recently, different applications of the scanning tunneling microscope (STM) and atomic force microscope (AFM) have been developed to observe these electrical quantities with nanometer resolution, allowing a better understanding of the silicon device operations. Each of these electrical characterization tools fulfills one or more of the requirements imposed by current and future silicon processing technologies: spatial resolution, accuracy, sensitivity, dynamic range of the electrical measurement, measurement speed, ease of transforming data into physical properties of interest. The surface potential distribution can, for example, be measured by contactless techniques such as scanning Kelvin probe microscopy (Nonnenmacher et al., 1991) and scanning tunneling potentiometry (Muralt and Pohl, 1986). Contact mode AFM has been used for the potential mapping inside silicon devices under operation (Trenkler et al., 1995; Uchihashi et al., 1994). The carrier concentration profile can be determined by scanning capacitance microscopy (Huang et al., 1995), scanning resistance microscopy (Nxumalo et al., 1996), scanning tunneling spectroscopy (Yu et al., 1996), nano-spreading resistance profiling or nano-SRP (De Wolf et al., 1996), and dopant selective etching followed by AFM imaging (Barrett et al., 1996; Raineri et al., 1994). A recent overview is given by Dagata and Kopanski (1995).

In this work, an AFM equipped with a conductive probe is used in the contact mode to measure both the carrier concentration and potential distribution. In the first method, named nanopotentiometry, the electrical potential on the sample cross-section is monitored with a conductive probe, concurrent with the cantilever deflection, while the probe is scanned across the sample cross-section at a predetermined force. In this way, topographical and potentiometric images of the interior of
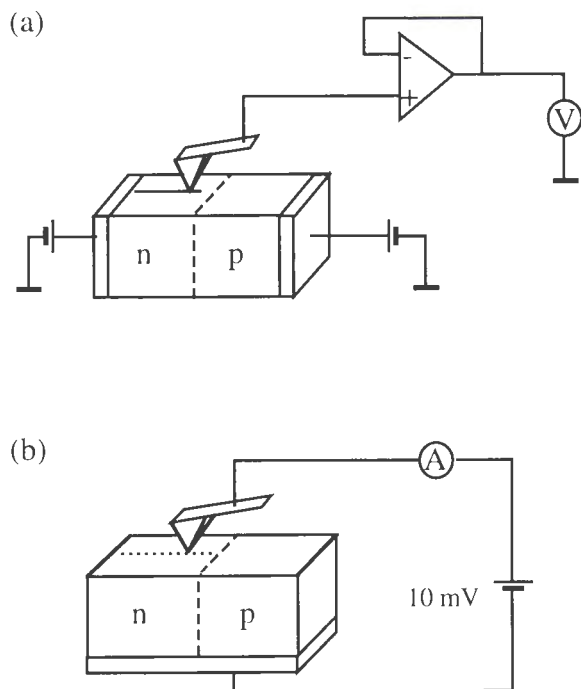
(a)

(b)

Figure 1. Schematic representations of (a) the potential measurement setup and (b) the nano-SRP setup.

---

the device are being recorded simultaneously with nanometer resolution. A second method, using the same set-up and named nano-SRP, determines the resistivity (and consequently, the carrier) distribution in silicon devices by performing localized resistance measurements, while the conductive probe is stepped across the sample. Doped diamond and doped diamond coated silicon probes were found to withstand the high mechanical and electrical stresses which are inherent to both operation modes. All measurements were performed on the cross-section of silicon devices, under ambient conditions.

Experimental Procedures

Local potential measurements and nano-SRP setup

In the first method, the electrical potential distribution inside a silicon device under operation (i.e., with the necessary voltages applied) is imaged. Figure 1a shows a schematic representation of the basic setup needed for the measurement of the potential distribution on a (reverse biased) *pn* junction. The potential distribution inside the silicon device is measured by a conductive AFM probe which is connected to a high input impedance voltmeter (10^{14} Ω). The repulsive force between the probe and the silicon sample is held constant by the AFM feedback loop, while the probe is scanned across the silicon sample. In this way, the surface topography is mapped. This allows the potential distribu-

tion to be determined with respect to other device characteristics such as mask edges, gate oxide, spacers or metallization layers.

Figure 1b shows the nano-SRP setup in detail. Here, the resistance is measured between a conductive AFM probe and a large current-collecting back-contact, while the probe steps across the cross section of the silicon device. When the applied force exceeds a certain threshold force, the measured resistance is dominated by the spreading resistance, which is dependent on the local carrier concentration underneath the probe-silicon contact (De Wolf *et al.*, 1996). Because of the high stresses applied, the force is decreased as much as possible when the probe is moved from one location to the next, in this way reducing the risk of damaging the probe. Consequently, no topography is obtained. The resistances are determined by measuring the current flowing through the probe at 10 mV bias as in conventional SRP. Since the current is proportional to the local carrier concentration, it may vary by several orders of magnitude when a silicon device is measured (typically from 10^{-5} to 10^{-11} A) and a high-performance current meter is required.

Sample and probe preparation

For both techniques presented, the same sample preparation is used. First, a cross section cutting through the silicon device of interest is made by cleaving or polishing. Second, all electrical contacts are attached to the sample by ultrasonic soldering or wire bonding. Note that the nano-SRP technique needs only one (large) current collecting contact, while two or more contacts are needed when one wants to map the potential distribution. Finally, all samples are cleaned ultrasonically in isopropyl alcohol and deionized water. No special treatment was carried out in order to remove the native oxide or passivate the silicon.

Two types of conductive AFM tips are used: boron doped diamond probes and doped silicon tips coated with a thin layer of chemical vapor deposited (CVD) doped diamond (Niedermann *et al.*, 1996). The conductivity of some of the diamond probes was further improved by deposition of a thin tungsten layer (40 nm). Cantilever spring constants varied between 1 and 300 N/m. Diamond is used so that the tips can withstand the mechanical forces while scanning in contact mode. Metal tips and metal-coated silicon or silicon nitride tips showed insufficient life-time for these applications. Care is taken that no external light or laser light (originating from the AFM deflection detection) falls on the silicon device and distorts the electrical measurement. All measurements were carried out on a commercial Nanoscope III AFM (Digital Instruments Inc., Santa Barbara, CA).
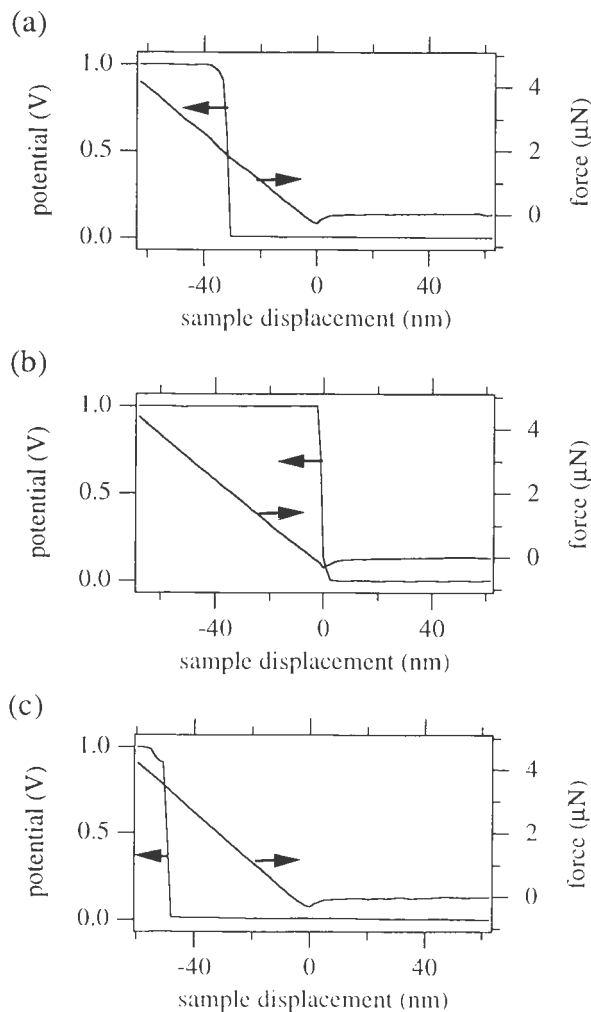
(a)

(b)

(c)

Figure 2. Force profile and measured potential on **(a)** a bulk silicon sample, **(b)** a Pt sample, and **(c)** a bulk Si sample with a 4.6 nm oxide layer. A diamond-coated Si tip was used on a cantilever with a spring constant of 68.5 N/m.

Results and Discussion

Potential mapping

The forces needed for reproducible potential measurements on silicon devices under ambient conditions are determined by measuring force profiles while a fixed voltage is applied to the sample. The voltage on the tip is monitored simultaneously with the force profile, which shows the force acting on the tip as a function of tip-sample distance. Figure 2a shows a force profile in combination with the measured potential for a homogeneously doped silicon sample under a bias of 1 V. A diamond-coated silicon probe with a spring constant of 68.5 N/m was used. The data for increasing tip-sample distances (withdrawal) are omitted. When the probe
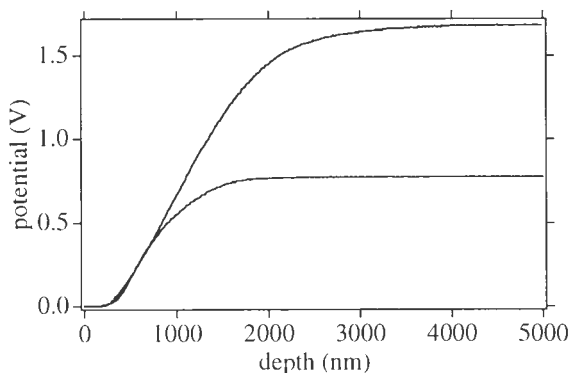

Figure 3. One-dimensional potential measurement over an abrupt *pn* junction under a reverse bias of 0.8 V (bottom curve) and 1.7 V (top curve).

---

jumps into contact with the silicon sample (distance 0 nm), the measured potential is still 0 V. The tip potential jumps to 1 V when the tip-sample force is further increased by lifting the sample towards the probe. A similar response was observed when the bias voltage on the sample was decreased to values as low as 1 mV. As discussed previously by O'Shea *et al.* (1995), there are two ways to explain this behavior. First, the very apex of the tip might not be conducting. Second, a thin insulating layer on the tip or sample may be present, through which tunneling can occur, only when the force is increased. Similar curves measured with the same probe on a Pt sample (Fig. 2b) exclude the first explanation and indicate that the extra sample displacement needed can be entirely attributed to the native oxide (and any other insulating contaminants) on top of the silicon sample. When using the same probe on a silicon sample on which an oxide layer (thickness 4.6 nm) was grown, the extra sample displacement needed for potential measurements further increases (Fig. 2c). Since the thickness and the quality of the native oxide on a cleaved or polished cross section are not constant, the force chosen for reliable potential measurements is a little higher than the threshold determined by the present method. All probes are inspected in this way both before and after scanning, to ensure that the electrical properties of the tip are not altered during the measurement.

To illustrate the strength of this method, one-dimensional measurements were performed on an abrupt *pn* junction which had been prepared by epitaxial deposition of a boron-doped layer (1×10^{17} atoms/cm^3) on an *n*-type substrate with a doping level of 1×10^{15} atoms/cm^3. Contacts were ultrasonically soldered at the front and back side of the sample. An ion-implanted diamond tip was used at a force of 7 μN. Figure 3 shows the potential distributions measured when either
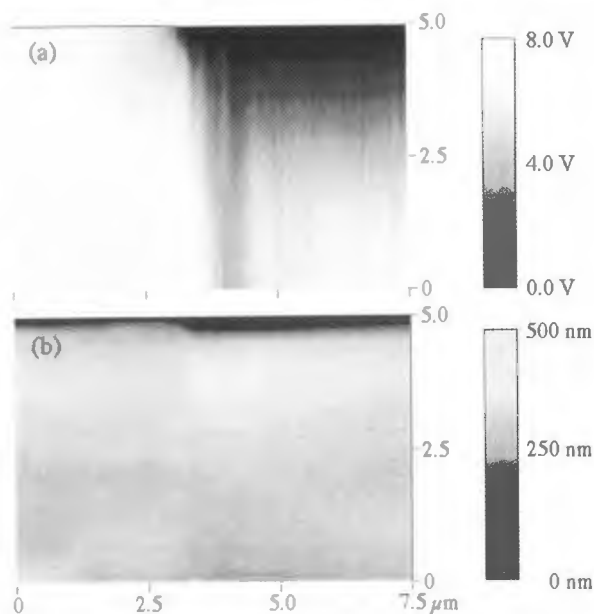
Figure 4. (a) Potential distribution inside a two-dimensional junction under 8 V reverse bias, measured with a ion-implanted diamond AFM probe in contact mode. (b) Corresponding topographic image showing the masked region on the left, the implantation window on the right.

0.8 V or 1.7 V reverse bias is applied across the junction. One can clearly observe the potential drop across the depletion zone and its extension into the (lowly doped) *n*-type substrate for higher voltages.

Figure 4 shows the surface topography and potential distribution simultaneously measured on a two-dimensional silicon diode under a reverse bias of 8 V. The diode was made by a 20 keV boron implantation (2 x 10^{15} atoms/cm^2) into an *n*-type substrate, through a SiO$_2$ stripe pattern (10 μm alternating mask and window), followed by an annealing step (30 minutes, 900°C). One large contact was soldered to the substrate, another wire-bonded to the window area contacting the implantation zone. The topographical image (Fig. 4b) clearly shows the edge of the implantation mask, while the potential image (Fig. 4a) reveals the two-dimensional extension of the depletion zone in detail.

Since the potential measurement is performed on a device under operation, the electrical characteristics of the device (for example, junction leakage currents) might be disturbed when the conductive probe is brought into contact with the cross section of the device. Therefore, the electrical characteristics were monitored while the potential mapping was performed. No change in leakage current was observed during the potential measurements on the junctions, presented in Figures 3 and 4. On the
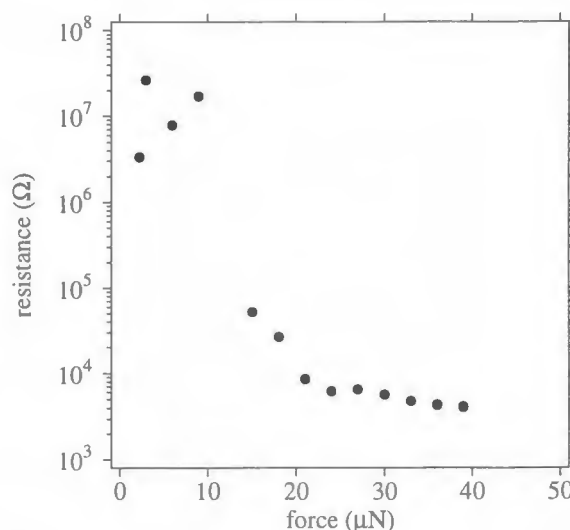

Figure 5. Measured resistance on bulk silicon (*p*-type, 0.01 Ωcm) as a function of force. A CVD diamond-coated silicon probe was used.

----

other hand, the device characteristics might be changed because of the sample preparation steps needed to expose the inner structure of the silicon device. Not only is the active area smaller after partial removal of device material, but also a large number of surface states are introduced on the cross section, possibly leading to increased leakage current. Consequently, the probe is not imaging the original voltage distribution inside the device (before sample preparation), but a voltage distribution which is influenced by the presence of the cross-section through the device. Further study will be required to specify the importance of this effect and its influence on the potential distribution which is being recorded. For the case of a simple *pn* junction, it has already been demonstrated that the experimental results are in close agreement with theoretical predictions (Trenkler *et al.*, 1995).

Nano-SRP

The minimum force needed for reliable resistance measurements can be determined in a similar way, as is done for nanopotentiometry. For this purpose, the resistance is measured while the force acting on the probe is increased by changing the AFM feedback setpoint. Figure 5 shows the resistance measured on a uniformly doped sample (*p*-type, 0.01 Ωcm) plotted as a function of the applied force for a diamond-coated silicon probe. A large change in resistance is observed when the force exceeds 10 μN. When measuring on different uniformly doped samples at forces below this transition force, no correlation between resistance and carrier concentration
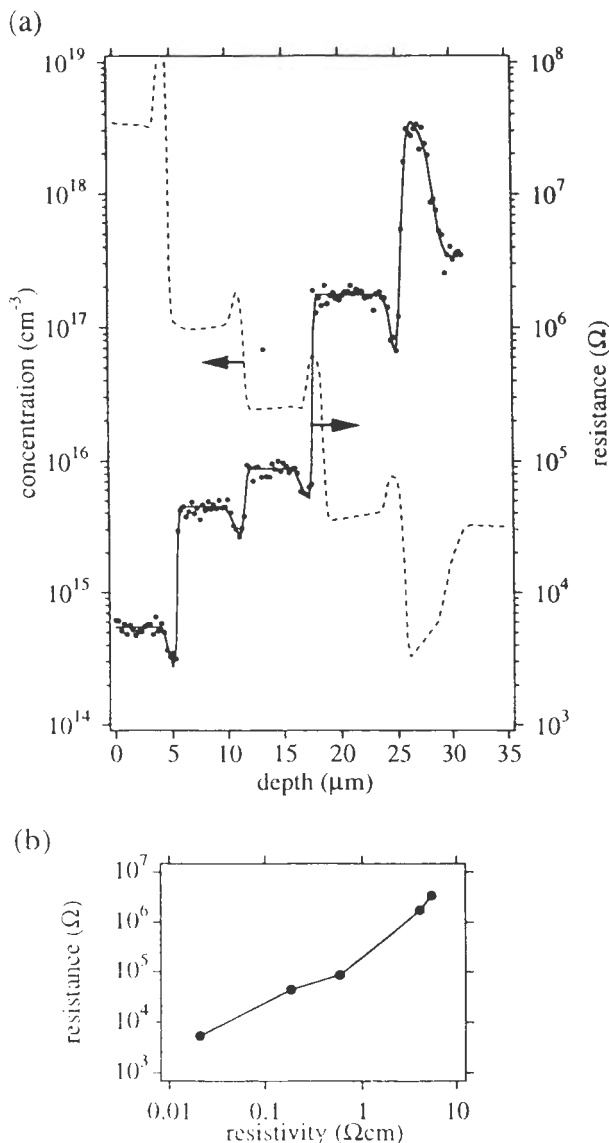
(a)

(b)

Figure 6. (a) Nano-SRP profile measured with a W-coated doped diamond probe (at 90 μN) on a p-type epitaxially grown staircase calibration sample. The filled circles show the raw resistance data while the full line shows the smoothed data. The dashed line shows the carrier concentrations as derived from conventional SRP. The resulting calibration curve is shown in (b).

----

is observed. Once above the transition force, the measured resistance increases monotonically with sample resistivity and can therefore be used for carrier profiling. Higher forces are required for nano-SRP than for potential measurements (Fig. 3). Also, plastic deformation of the sample is observed only if the threshold force is exceeded. Hence, one may conclude that the plastic deformation, which is accompanied by a pressure-driven phase transformation of the silicon into a b-Sn structure

with metal-like electrical properties (Clarke *et al.*, 1988), is necessary. As a consequence of the high forces, the contact size is much larger (typically 30 nm radius) than for conventional contact mode AFM (Snauwaert *et al.*, 1996). Obviously, this sets limits to the range of materials and spring constants of the probes suited for nano-SRP.

As with conventional spreading resistance profiling (SRP), an n-type and p-type calibration curve, showing the relation between the resistivity and the measured (spreading) resistance values for a range of resistivity values, is needed for nano-SRP. Typical nano-SRP calibration curves, obtained by using a set of homogeneously doped silicon samples, were already presented in earlier work (De Wolf *et al.*, 1996). In order to improve and speed up the inevitable calibration process, special samples were prepared. These samples (one n-type and one p-type) are composed of a stack of epitaxially grown layers each with a constant carrier concentration. The stack covers the entire concentration calibration range (10^{15}-10^{20} atoms/cm^3). A typical example, obtained with conventional SRP measurements is shown by the carrier profile in Figure 6a. A nano-SRP resistance profile, measured on the cross-section of the sample is also shown in Figure 6a. The profile was measured with a doped diamond probe at a contact force of 90 μN. The corresponding p-type calibration curve, obtained by plotting the measured resistance levels versus the resistivity levels, is shown in Figure 6b. This figure illustrates that the nano-SRP is sensitive and has a high dynamic range compared to other AFM-based carrier profiling techniques.

When measuring a one- or two-dimensional carrier profile by nano-SRP, direct interpolation of the calibration data can in principle be used to convert the measured resistance values into local resistivity values. However, when measuring on the cross-section of a sample, other regions of the profile (containing different carrier concentrations) are very near. Current might be mainly carried through the highly doped parts of the profile leading to a decrease in resistance. Data points in poorly doped regions or in the proximity of a junction will be particularly sensitive to this effect. Hence, there is a need to introduce a correction factor, denominated α, taking this effect into account. The measured resistance on a non-homogeneous sample at a position x_0 is then given by, $R(x_0) = \alpha \cdot R_{bulk}$, where R_{bulk} represents the resistance measured on a semi-infinite bulk sample with a concentration equal to the one at position x_0, and α, a factor correcting for the current spreading. The correction factor α will depend on (i) the shape of the carrier profile, (ii) the probe radius, and (iii) the distance to insulating or conducting boundaries. The evaluation of the importance of the current spreading effect
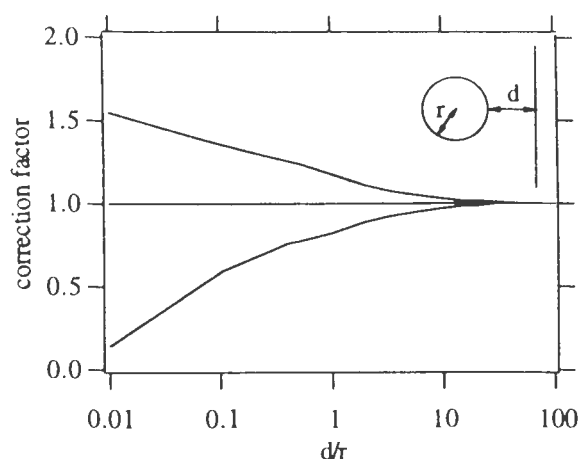
Figure 7. Nano-SRP correction factors for a homogeneously doped sample as a function of the distance to an ideal conducting (bottom curve) and isolating (top curve) boundary. The results were obtained by 3D finite element device simulations.

----

requires a detailed three-dimensional calculation of the current distribution around the nano-SRP point contact, ultimately leading to a deconvolution algorithm which translates the measured resistance profile into the exact carrier profile. A 3D device simulation package (DESSIS, ISE Integrated Systems Engineering AG, Zurich, Switzerland) was used to calculate the variation of α for homogeneously doped samples as a function of the distance to an ideal conducting or insulating boundary (Fig. 7). The effect of the probe radius was taken into account by scaling the distance to the boundary with the probe radius. Several conclusions can be drawn from Figure 7. First of all, the correction factor α seems to be limited to values between 0.1 and 2 for reasonable distances. Secondly, although the appearance of a boundary (in particular, a conductive one) near the probe has a strong influence on the value of the correction factor, its effect dies out quickly when the probe is moved away from the boundary. Third, decreasing the size of the contact radius will decrease the sampling volume, and thus reduce the effect of nearby layers. Based on these correction factors, a detailed correction algorithm was constructed which allows transformation of the measured resistance profile into the exact carrier profile (De Wolf *et al.*, in preparation).

Figure 8a shows the contour lines of a two-dimensional concentration profile. The sample used was prepared by a double implantation (As: 5 x 10^{15} atoms/cm^2, 80 keV and P: 5 x 10^{14} atoms/cm^2, 50 keV) through a regular stripe pattern (300 nm thick, 0.7 μm alternating mask and window) into an *n*-type substrate with concentration 3 x 10^{14} atoms/cm^3. The sample was

annealed for 21 seconds at 1020°C. A 3 μm polysilicon cap layer was deposited on top of the structure. It took about 30 minutes to perform the nano-SRP resistance measurements on a 50 nm spaced grid covering an area of 2 μm x 0.5 μm. No contour lines were obtained for concentrations above 5 x 10^{17} atoms/cm^3 because the particular diamond probe used in this experiment showed insufficient conductivity (checked on a Pt sample) limiting the dynamic range in this experiment (De Wolf *et al.*, 1996). The carrier depth profile, as obtained by conventional SRP on a larger structure, is shown in Figure 8b. The result of a dopant selective etch followed by AFM topographic imaging of the same structure is represented in Figure 8c. The etching conditions (HNO$_3$:HF:H$_2$O 1:3:8 by volume, no light, T = 21°C, 10 seconds) expose the carrier profile down to a level of 10^{19} atoms/cm^3 (Raineri, 1994). From Figure 8, it is clear that none of the three techniques (SRP, nano-SRP or selective etching) is presently capable of measuring the two-dimensional carrier profile, with nanometer resolution, high sensitivity and over a high dynamic range (10^{14}-10^{21} atoms/cm^3). The conventional SRP technique is limited to one-dimensional profiles. The chemical delineation combined with AFM imaging provides the most visual information but lacks sensitivity and dynamic range. The nano-SRP technique is by far the more sensitive, quantitative and reproducible of the three, although at present, it is limited in spatial resolution by the 30-50 nm contact radius required by the force threshold, and in dynamic range by the conductance of the probe. Elimination of native oxide on the samples and further tip improvement will alleviate the minimum force requirement and improve the resolution and dynamic range.

Conclusions

The AFM, equipped with a hard conductive probe is emerging as an appropriate tool for the electrical characterization of silicon devices. The characterization is performed on the cross section of the devices under investigation, allowing measurements inside the device. The nano-SRP is a sensitive, easy to quantify carrier-profiling technique. Data interpretation is straightforward when calibration curves, measured on specially prepared samples, are used in combination with a newly developed deconvolution scheme. The electrical potential mapping by AFM in the contact mode is a complementary method, providing extra information on the detailed functioning of the device. In addition, it is a truly scanning technique, providing a combined image of topography and electrical potential distribution. The low forces required as compared to nano-SRP allow smaller contacts and higher spatial resolution (< 10 nm).
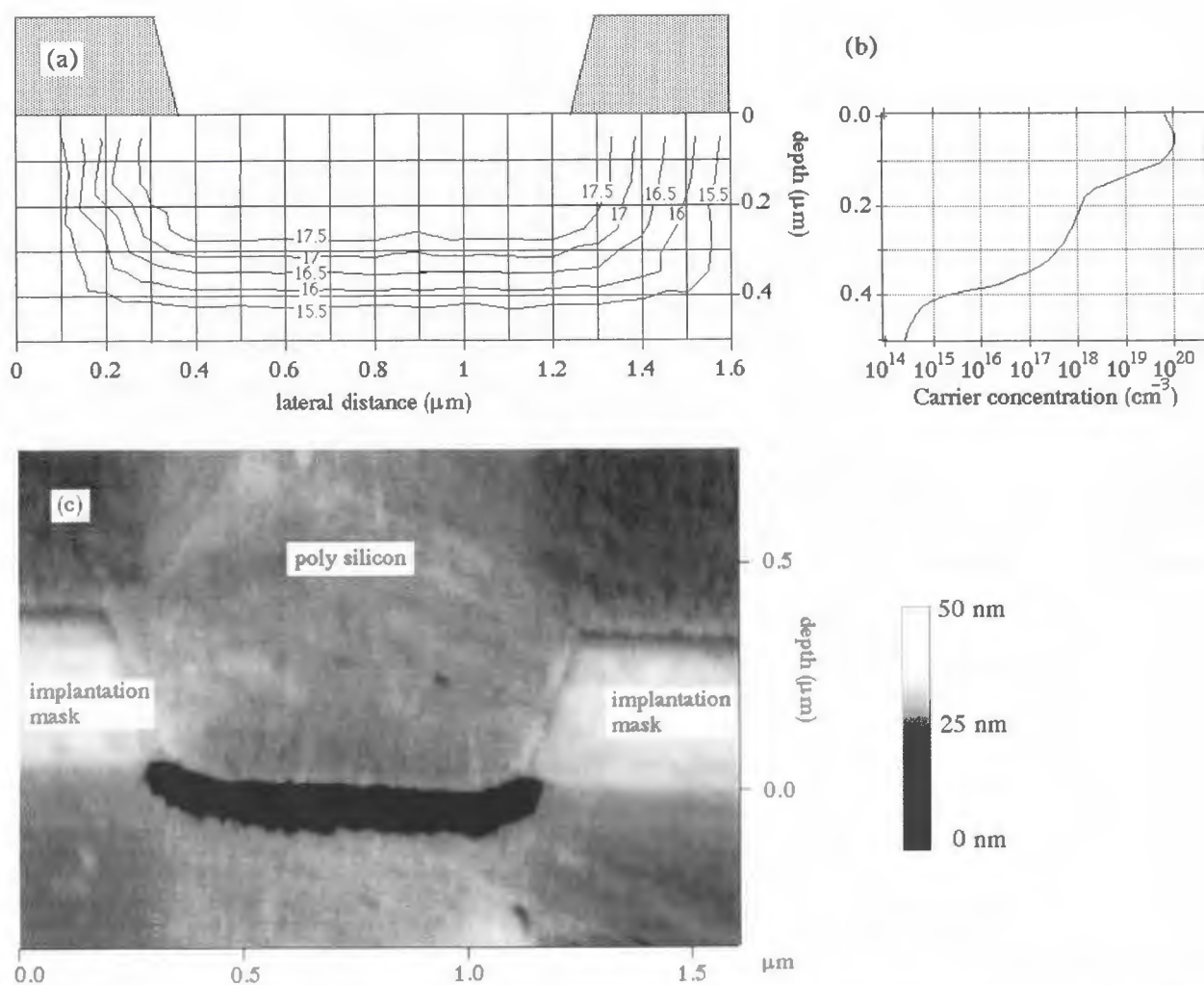
Figure 8. (a) Contour lines of a two-dimensional carrier profile measured with nano-SRP. In (b) the in-depth carrier profile is shown as obtained from conventional SRP measurements for the same implantation conditions. The topography imaged with AFM after exposing the same structure to a dopant selective etch is shown in (c). The dark area corresponds to carrier concentrations larger than 10^{19} atoms/cm^3.

References

Barrett M, Dennis M, Tiffin D, Li Y, Shih CK (1996) Two-dimensional dopant profiling of very large scale integrated devices using selective etching and atomic force microscopy. J Vac Sci Technol B **14**, 447-451.

Clarke DR, Kroll MC, Kirchner PD, Cook RF, Hockey BJ (1988) Amorphization and conductivity of silicon and germanium induced by indentation. Phys Rev Lett **60**, 2156-2159.

Dagata JA, Kopanski JJ (1995) Scanning probe techniques for the electrical characterization of semiconductor devices. Solid State Technol, July, 91-97.

De Wolf P, Clarysse T, Vandervorst W, Snauwaert J, Hellemans L (1996) One- and two-dimensional carrier profiling in semiconductors by nanospreading resistance profiling. J Vac Sci Technol B **14**, 380-385.

Huang Y, Williams CC, Slinkman J (1995) Quantitative two-dimensional dopant profile measurement and inverse modelling by scanning capacitance microscopy.

Appl Phys Lett **66**, 344-346.

Muralt P, Pohl DW (1986) Scanning tunneling potentiometry. Appl Phys Lett **48**, 514-516.

Niedermann Ph, Hänni W, Blanc N, Cristoph R, Burger J (1996) Chemical vapor deposition diamond for tips in nanoprobe experiments. J Vac Sci Technol A **14**, 1233-1236.

Nonnenmacher M, O'Boyle MP, Wickramasinghe HK (1991) Kelvin probe force microscopy. Appl Phys Lett **58**, 2921-2923.

Nxumalo JN, Shimizu DT, Thomson DJ (1996) Cross-sectional imaging of semiconductor device structures by scanning resistance microscopy. J Vac Sci Technol B **14**, 386-389.

O'Shea SJ, Atta RM, Welland ME (1995) Characterization of tips for conducting atomic force microscopy. Rev Sci Instrum **66**, 2508-2512.

Raineri V, Privitera V, Vandervorst W, Hellemans L, Snauwaert J (1994) Carrier distribution in silicon devices by atomic force microscopy on etched surfaces. Appl Phys Lett **64**, 354-356.

Snauwaert J, Blanc N, De Wolf P, Vandervorst W, Hellemans L (1996) Minimizing the size of force-controlled point-contacts on silicon for carrier profiling. J Vac Sci Technol B **14**, 1513-1517.

Trenkler T, De Wolf P, Snauwaert J, Qamhieh Z, Vandervorst W, Hellemans L (1995) Local potential measurements in silicon devices using AFM with conductive tips. In: Proceedings of the European Solid State Device Research Conference 1995, The Hague, The Netherlands. de Graaff HC, van Kranenburg H (eds.). Editions Frontieres, Gif Sur Yvette, France. pp. 477-481.

Uchihashi T, Fukano Y, Sugawara Y, Morita S, Nakano A, Ida T, Okada T (1994) Potentiometry combined with AFM. Jpn J Appl Phys **33**, L1562-L1564.

Yu ET, Barmak K, Ronsheim P, Johnson MB, McFarland P, Halbout JM (1996) Two-dimensional profiling of shallow junctions in Si metal-oxide-semiconductor structures using scanning tunneling spectroscopy and transmission electron microscopy. J Appl Phys **79**, 2115-2121.

Discussion with Reviewers

C.-K. Shih: The local potential mapping is very interesting. It is nice to see that the potential distribution of a *pn* junction under reverse bias can be mapped out in real space. I presume one of the keys to this technique is the use of a very high input impedance (10^{14} Ω) voltmeter in order not to disturb the potential distribution by the probe itself. The ultimate challenge of this technique is to see if it can be used to map out the two-dimensional potential distribution in an ultra-shallow junction.

Unfortunately, the dimension of the device being used in this study is rather large, and it is hard to assess the ultimate potential of this technique. Please comment.

D.J. Thomson: Figure 4a is a potential map of a *pn* junction. There is some streaking of the potential in this image that seems hard to understand.

Authors: The experiments illustrate the one- and two-dimensional capabilities of the local potential mapping technique. In Figure 4, the probe moved up and down over the edge of the sample cross section in the implanted region, but did not go over the edge in the thicker, masked region. Potential mapping was severely affected by topography in the transition zone between both regions, resulting in the streaks. When the scan direction was rotated by 90 degrees, no streaking of the potential was observed.

Ultra-shallow structures demand even more careful sample surface preparation and need wires to be attached to the different parts of the device in order to apply the necessary voltages. Future experiments will help to assess the ultimate resolution of this technique, which we believe to be limited only by the size of the probe/sample contact. In this work, the contact was estimated to have a diameter of 40 nm (by point contact measurements on uniformly doped samples). Further improvement of the tip geometry is required to reduce this to a smaller value.

D.J. Thomson: What type of current meter was used for the measurement of 10^{-11} A currents in nano-SRP? What is the noise level in the measurement of these small currents?

Authors: In the nano-SRP technique, a Keithley 237 source/measure unit (Keithley Instruments, Inc., Cleveland, OH) was used with a resolution of 10^{-14} A. For optimum performance, a special test fixture providing guarding and shielding should be used. In our setup, currents as low as 10^{-10} A were measured with a noise level of 10^{-11} A.

C.-K. Shih: I am somewhat confused regarding the dynamic range of the nano-SRP work. In the measurement of the two-dimensional carrier profile on the test device (Fig. 8), the authors mentioned that no contour lines were obtained for concentrations above 5×10^{17} atoms/cm^3 because the diamond probe being used showed insufficient conductivity, limiting the dynamic range. On the other hand, in their measurement of a one-dimensional carrier profile on the epitaxial layer (Fig. 6), they clearly show the ability to measure carrier concentrations up to 10^{19} atoms/cm^3. Please comment.

Authors: The conductivity of the nano-SRP probes varied from probe to probe. Therefore, some of the probes were coated with a thin layer of tungsten (40 nm), which

improved the dynamic range considerably. The particular probe used for the two-dimensional measurement unfortunately was not conducting as well as the one used for the one-dimensional work.

M.D. Johnson: The authors mention scanning tunneling potentiometry (STP) as a technique capable of measuring carrier profiles, but fail to discuss the fact that this technique has been successfully used to measure silicon devices. Ultimate sensitivity, resolution, and reproducibility should be addressed and contrasted with the work of this paper. I believe, like the authors, that to date there is no clear winner.

Authors: Using the scanning tunneling spectroscopy (STS) technique (Yu *et al.*, 1996), silicon structures such as *pn* junctions can be characterized by measuring localized current-voltage spectra. Qualitative differences in measured STS spectra for *n*-type and *p*-type material were found to be consistent with theoretical simulations and are used to delineate depleted layers, *n*-type and *p*-type material regions with nanometer-scale spatial resolution. A problem encountered while extending the STS work to actual profiling is the dependence of the tunneling current on the Fermi-level, rather than on the carrier concentration. Since the former scales with the logarithm of the concentration, the sensitivity of the STS-approach to subtle profile variations is limited. In the nano-SRP technique, the measured resistance linearly scales with the resistivity of the underlying material, resulting in a high sensitivity and a high dynamic range as illustrated by the calibration curves. The ultimate spatial resolution of the nano-SRP technique is limited by the size of the probe/sample contact. At present, it is not clear whether conductive probes can be made with a smaller contact radius which are hard enough to withstand the high stresses involved in the nano-SRP.

Authors' late addition: The reference mentioned in text as "De Wolf *et al.*, in preparation" has now been accepted for publication, the bibliographic details are: De Wolf P, Clarysse T, Vandervorst W (1998) Quantitative nanospreading resistance profiling. J Vac Sci Technol B, accepted for the Jan/Feb 1998 issue.